Int. J. Heat Mass Transfer. Vol. 15, pp. 2045–2062. Pergamon Press 1972. Printed in Great Britain

THE INFLUENCE OF CURVATURE IN POST DRY-OUT HEAT TRANSFER

MAURIZIO CUMO, GIOVANNI ELVIO FARELLO and GIUSEPPE FERRARI
Comitato Nazionale per l'Energia Nucleare, Centro di Studi Nucleari della Casaccia, Roma, Italy

(*Received* 13 *July* 1971 *and in revised form* 1 *December* 1971)

Abstract—Post burnout heat transfer has been investigated comparatively in straight and coiled tubes, in order to study the influence of the geometric parameter. Freon 12 has been employed, up to supercritical pressures.

An improved two-phase flow heat transfer has been discovered in coiled than in straight ducts: higher burn-out heat fluxes, smoother and lower wall temperature rises at the dry-out point. In post burnout heat transfer a wall temperature difference between the internal and the external side of the coil (with respect to the helix axis) is set up.

This temperature difference remains almost constant with quality downward from the dry-out point, depends on flow centrifugal acceleration and pressure, and remains at moderate values up to supercritical pressures.

NOMENCLATURE

d_{tube}, inner diameter of the tube;
D_{coil}, diameter of the coil;
G, specific mass flowrate;
Nu, Nusselt number;
p, pressure;
Pr, Prandtl number;
R_{coil}, radius of the coil $= D_{coil}/2$;
Re, Reynolds number;
Sl, slope of the wall temperature profile after the dry-out point, $= \theta T/\theta z$;
X, quality;
X, abscissa along the test section;
$\Delta T_{B.O.}$, wall temperature rise at the dry-out point;
ΔT_{os}, difference in the wall temperatures between two opposite sides in the coil;
ϕ, surface heat flux;
π, reduced pressure (p/p_{cr});
ρ, density;
W, thermal power;
T, temperature.

Suffixes

B.O. burn-out or dry-out point;
cr, critical;
f, film;
l, liquid;
m, mixture;
sat, saturation;
v, vapour;
w, wall;
b, bulk.

REVIEW OF THE EXISTING LITERATURE

HEAT transfer in coiled tubes has been studied rather sporadically and with few geometries, mainly with gases and water in single phase flow. A few measurements in two-phase flow have been recently made, disclosing very interesting results.

In the helical flow through a coiled tube there

are centrifugal forces and body forces due to gravity, which have a separating effect, due to the differences in density, in the case of a two-phase flow. There is also a spiraling secondary flow, which is superimposed on the primary flow, following the helicoidal axis.

In a two-phase flow, the presence of secondary flow counteracts the separating effects of the phases and tends to make the mixture uniform for all azimuthal locations in the cross section of the coiled tubes. The azimuthal pressure distribution within the cross section (Fig. 1) is

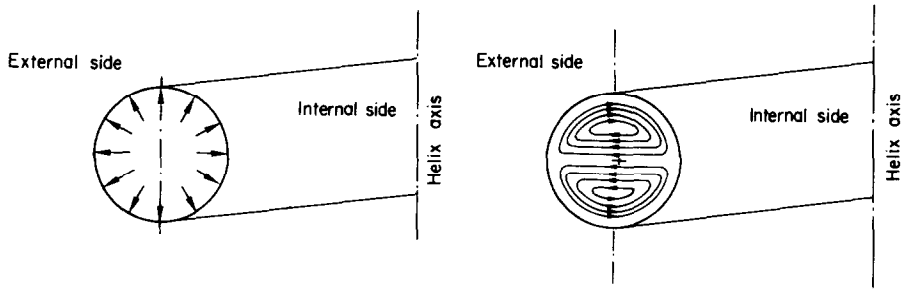

FIG. 1. Sketch of the azimuthal pressure distribution and the secondary flow within a coiled tube.

not uniform, due to the centrifugal effect, and the secondary flow, transverse to the main flow, follows loop lines (Fig. 1) which bring coolant from the external side to the internal side of the coil, thus counteracting the centrifugal field.

The relative importance of the two separating effects (centrifugal and gravity force) in a two-phase flow depends, obviously, on the specific mass flowrate: buoyancy forces would be felt more at lower mass velocities, due to less turbulence.

A precise description of the flow field in a diabatic flow is very difficult even for a single phase fluid. The difficulty is enormously increased for a two-phase fluid, and a basic insight into the phenomenon would be of great help.

The most complete analytical treatise of a single phase, helical, turbulent flow comes from Y. Mori and W. Nakayama [1]. The Nusselt numbers obtained from measurements of the velocity and temperature distributions in an air flow through curved pipes are in good agreement with the theoretical results. They show that the secondary flows cause a larger amount of pressure drop and heat transfer rate than those for straight pipes, and, furthermore, that the effect of curvature is far less evident in a turbulent flow than in a laminar flow.

For single-phase, turbulent flow, McAdams [2] cites the results of Jeschke for air in curved tubes, for which the heat transfer coefficient exceeded that for a straight tube, at the same Reynolds number, by the factor:

$$1 + 3{\cdot}5\frac{d_{\text{tube}}}{D_{\text{coil}}}.$$

Seban and McLaughlin [3], for the same situation of turbulent flow (water) have deduced, within ± 5 per cent of experimental error, the following empirical correlation:

$$Nu = 0{\cdot}023\, Re^{0{\cdot}8}\, Pr^{0{\cdot}4} \cdot \left[Re^{1/20} \left(\frac{d_{\text{tube}}}{D_{\text{coil}}} \right)^{1/10} \right]$$

where the fluid properties have to be evaluated at the film temperature.

Forced convection heat transfer appears slightly increased due to the superimposed rotational flow which enhances eddy diffusivities [4].

Considering two-phase flows, major contri-

butions come from [5–12]. From these references it appears that the main differences between coiled (vertical axis of the coil) and straight tubes are the following:

Departure from nucleate boiling (DNB)* in coiled tubes occurs at different vapour qualities for different positions around the circumference of the tube, whereas, for a straight vertical tube, DNB occurs around the complete circumference of the tube at one vapour quality [6, 9].

Coiled tubes have higher average DNB vapour qualities than do straight vertical tubes [5–12].

In the transition from nucleate boiling to film boiling (DNB) the surface temperature fluctuations are much lower [6].

Coiled tubes have some portion of the inside surface around the circumference of the tube operating under film boiling and adjacent surfaces operating under nucleate boiling for several dozen diameters along the length of the tube [9].

The rise of tube wall temperature accompanying DNB in a coiled tube is much smaller and more gradual than in a straight vertical tube [6].

Stratification in bubble flow can be expected through the coil; however the presence of nucleate boiling and of transverse circulation in the stream facilitates mass transfer in the flow to such an extent that sufficient wetting of the tube perimeter with water is ensured, until the inception of DNB [7, 8].

In post burnout† there is an increase in the heat transfer coefficient (in coiled tubes), due to the wetting of the tube walls by liquid drops. Apparently, in the presence of transverse circulation, the liquid drops suspended in the flow have a greater probability of reaching the walls than in straight tubes, where no intensive transverse circulation is present [7].

Increasing the specific mass flowrate, the point of inception of dry-out moves from the top side to the internal side (with respect to the helix axis) of the tube cross-section [9].

At the lowest pressures the inception of dry-out takes place almost at the same point throughout the periphery of the tube cross section (at the same quality); at the same surface heat flux, an increase of the flowrate corresponds to an increase of the peripheral dissymmetry of the dry-out front of inception [9].

Generally, in coiled tubes the heat transfer coefficients and the friction factors increase during the heating of the fluid and decrease during cooling, as the ratio d_{tube}/D_{coil} is increased [7].

The "entrance length" for heat transfer, beyond which heat transfer becomes assessed, is approximately proportional to the diameter of the coil and to the square root of the tube diameter [7].

Adiabatic two-phase flow experiments have shown that the ratio of two-phase to single-phase pressure drop for a coil is approximately equal to that for a vertical straight tube with the same fluid at the same mass flow and quality (for single phase flow in coils it has been established [12] that the frictional pressure drop is greater in coils than in tubes).

For practical designs the helical coil has the advantage that the centrifugal forces are controlling the phase distribution consistently throughout the systems. If straight tubes are used there is inevitably a change in direction which necessitates bends which introduce random changes in phase distribution, usually deleterious and furthermore extremely difficult to predict [12].

For the film boiling (post burnout) of water ($98 < p < 215$ bars; $10 < G < 200$ g/cm^2 s)

* DNB, burn-out, dry-out are terms employed indifferently in the paper as synonyms.

† Throughout the paper, the words "burn-out" and "dry-out" will be used indifferently, well understanding that "dry-out" is a smooth "burn-out" without destructive effects, downward from which in the heated duct begins the post burnout two-phase flow region, with dry heated walls.

Miropolski and Pikus [7] have suggested the following expression:

$$Nu_f = cRe''^{0.8} \cdot Pr_w''^{0.8} \cdot z$$

where:

$$Re'' = \frac{Gd_{\text{tube}}}{\mu_{v\,\text{sat}}}$$

$$z = y\left[X + \frac{\rho_{v\,\text{sat}}}{\rho_{l\,\text{sat}}}(1 - X)\right]^{0.8}$$

$$y = \frac{\rho_{l\,\text{sat}}}{\rho_{v\,\text{sat}}}\left[1 - \frac{\rho_{l\,\text{sat}} - \rho_{v\,\text{sat}}}{\rho_{l\,\text{sat}}} X^{0.2}\right]$$

$$c = 0.017\left(1 + 1.59\frac{d_{\text{tube}}}{R_{\text{coil}}}\right)$$

and where the physical properties in the vapor Prandtl number are evaluated at the wall temperature.

Finally, Owhadi, Bell and Crain [8], experimenting with water at atmospheric pressure, have found a complete wetting of the tube wall up to high qualities (99%), and attribute this to the secondary flow in the vapor core which exerts a drag on the liquid phase and forces it to flow to the surface closest to the helix axis.

OBJECTIVES OF THE PRESENT RESEARCH

Now, the aim of the present research is to give a systematic insight into heat transfer in a coil by comparison with heat transfer in a straight tube, having particular regard to heat transfer in post burnout at various pressures, up to the critical pressure.

We have seen in the literature review that there are two main counteracting factors which act in a post burnout mixture cooling a heated coil: the centrifugal force which tends to separate the two phases and the pressure which, increasing, tends to make the mixture uniform. Thus, these two factors have been chosen as the most representative parameters in post burnout heat transfer in coils (gravity force, in our applications, is 2 or 3 orders of magnitude less than the centrifugal force).

The ability of our experimental apparatus to vary the pressure (up to critical), the specific mass flowrate and the surface heat flux enhances the exploitation of many other physical aspects of the phenomena, besides the preceding reviewed aspects.

EXPERIMENTAL APPARATUS

The experimental apparatus consists mainly of a S.S. freon loop, referred to as CF1, an extensive description of which is available in [13].

It consists of the loop sketched in Fig. 2 whose main characteristics are the following:

maximum flowrate: 200 l/h
(flowrate is measured with an error of ±0·5 l/h)

maximum pressure: 70 kgf/cm²
(pressure is measured with an error of ±0·25 kgf/cm²)

maximum heating power: 10 kW, supplied as d.c.
with a maximum voltage of 20 V (the overall computed error in the determination of surface heat fluxes ranges from 5% to about 8%).

Test sections are two tubular ducts of the same tube (S.S., heated length = 200 cm; outlet dia. = 6·35 mm; inlet dia. = 4·75 mm) of which one is curved in a coil with a radius of 90 mm and placed with vertical axis (upward flow of the coolant) and the other is straight vertical (upward flow), both electrically heated.

The coil is placed within an insulated box and is instrumented by 20 chrome–alumel thermocouples, 0·5 mm in diameter, inserted in the holes in the tube wall and placed 10 cm away from each other on the two opposite sides of the coil (internal and external, see Fig. 3). So it is possible to have the wall temperature profiles along the internal and the external sides, to detect, in the case of temperature differences, the presence of centrifugation effects. A similar instrumentation, but only on one side, is placed on the straight test section.

The two test sections are mounted in parallel, in such a way that it is possible to reproduce the same inlet conditions of the coolant temper-

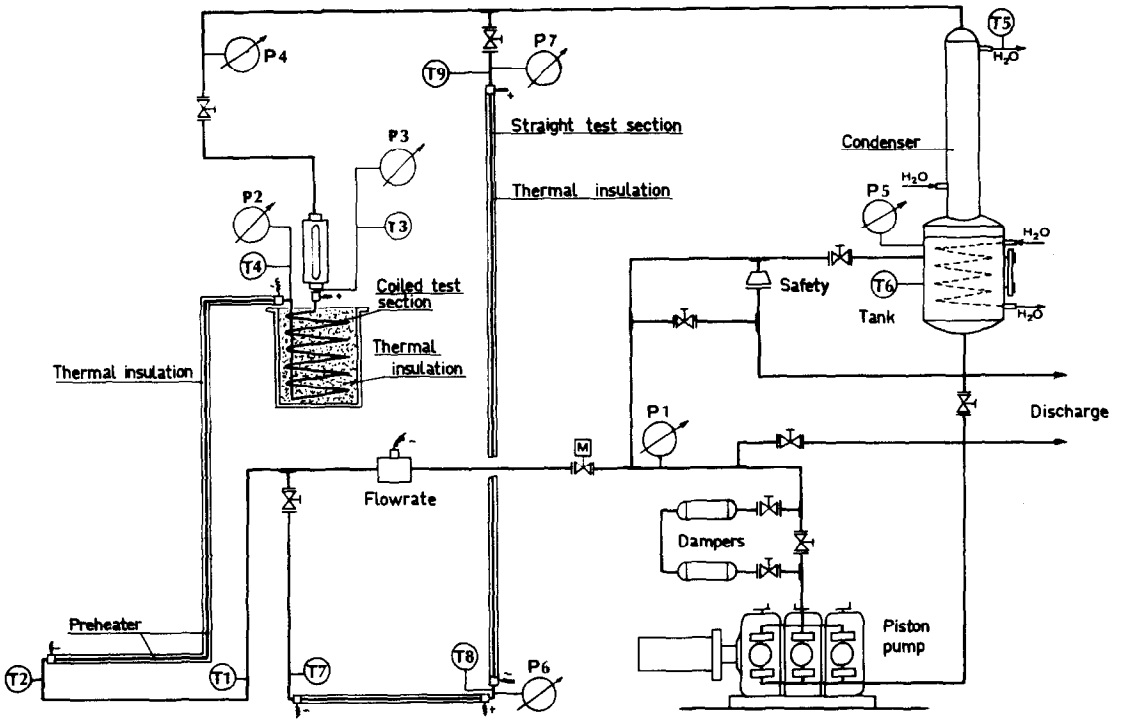

FIG. 2. Sketch of the experimental loop with the two test sections.

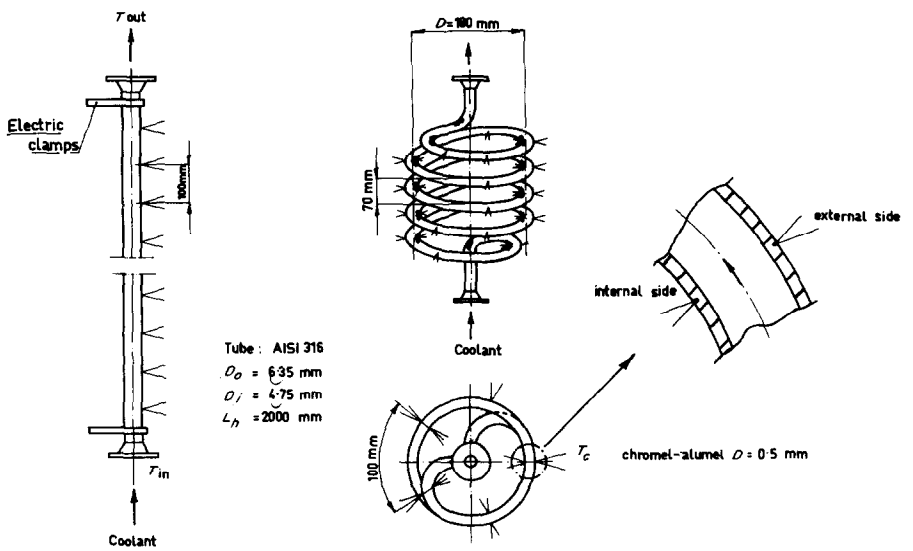

FIG. 3. Sketch of the straight and coiled test sections with the disposition of thermocouples.

ature, flowrate and pressure) and to inject the same heating power with the same surface heat flux, so that the geometry factor (curvature of the tube) is completely separated. Inlet and outlet temperatures are measured and recorded; so are the inlet and outlet pressures. Tempertures, flowrates, electric currents, voltage and pressures are all recorded in a data logger system. As coolant, Freon 12 has been selected for two main reasons: a good knowledge of physical properties [14] and low critical parameters (critical temperature: 111·5°C; critical pressure: 40·87 kgf/cm^2) and latent heat of vaporization.

The two test sections have been calibrated, calculating the heat loss through the external insulation at different temperature levels, and the wall thermocouples have been compared and calibrated in a similar way. Typical errors in the wall temperatures are of the $\pm 0{\cdot}5$°C.

A simple computer program has been set up to take account of the temperature distribution within the heated walls of the tube, to deduce finally the internal wall temperature T_w. Obviously this code takes into account the injected and dispersed thermal power, the variation of electric resistivity with temperature and the geometric variation of the external and internal wall thickness, due to bending. This last factor, particularly, induces a small variation in the external and internal wall heat fluxes. When the temperature differences between the two sides are studied, with respect to the centrifugal effects, the heat flux variations would induce an error. So we have measured directly, in this case, which are the temperature differences due to the heat flux differences, operating in single (liquid) phase, forced convection flow and have subtracted these temperature differences, in dependence on the heat flux levels, from the overall temperature differences, thus separating the centrifugal effects from the other, superimposed cause.

Magnified cross sections of the coil have been measured to deduce the geometric shape of the cross section itself.

Theoretical and experimental calibration agreed perfectly, and so the experimental program started. In every run, the heat flux profile along the test sections has been kept constant, injecting electric current through the two extremity clamps. Once the thermohydraulic conditions were stabilized, all the data were recorded. Different runs were obtained varying the pressure level, from a reduced pressure $\pi = p/p_{cr} = 0{\cdot}3$ up to a hypercritical pressure $\pi = 1{\cdot}1$. Independently, the specific mass flowrates were varied from $G = 50$ to $G = 180$ g/cm^{2}s, and also the heat flux ϕ, up to ~ 12 W/cm^2.

BURNOUT POWERS AND POST BURNOUT HEAT TRANSFER

Typical wall-temperature profiles are collected in the diagrams of Figs. 4–7. The diagrams of Figs. 4, 5 and 7 refer to subcritical conditions (i.e. $\pi < 1$), while the diagrams of Fig. 6 refer to critical ($\pi \simeq 1$) and supercritical ($\pi > 1$) conditions. Figure 7 contains a number of comparisons between straight and coiled tubes. Looking through the diagrams, first of all, it is evident that increasing the pressure and crossing the thermodynamic critical point the dry-out phenomenon disappears and no temperature jump occurs along the heated walls.

Another evident feature is the difference in wall temperatures which occurs after the dry-out point between the internal side (i.e. the side nearer to the helix axis) and the external side of the coil. This temperature difference constitutes one of the particular features of the coils in comparison with the straight ducts.

Downward from the dry-out point the temperature difference remains almost constant with the quality, so that it is characterised only, for a given coil, by the surface heat flux, the pressure and the specific mass flowrate. Even the dry-out point is not always at the same quality along the internal and external side of the coil, being anticipated in the internal side which, downward from the dry-out, is all at higher temperatures. Even at critical and supercritical pressures the two side temperatures remain

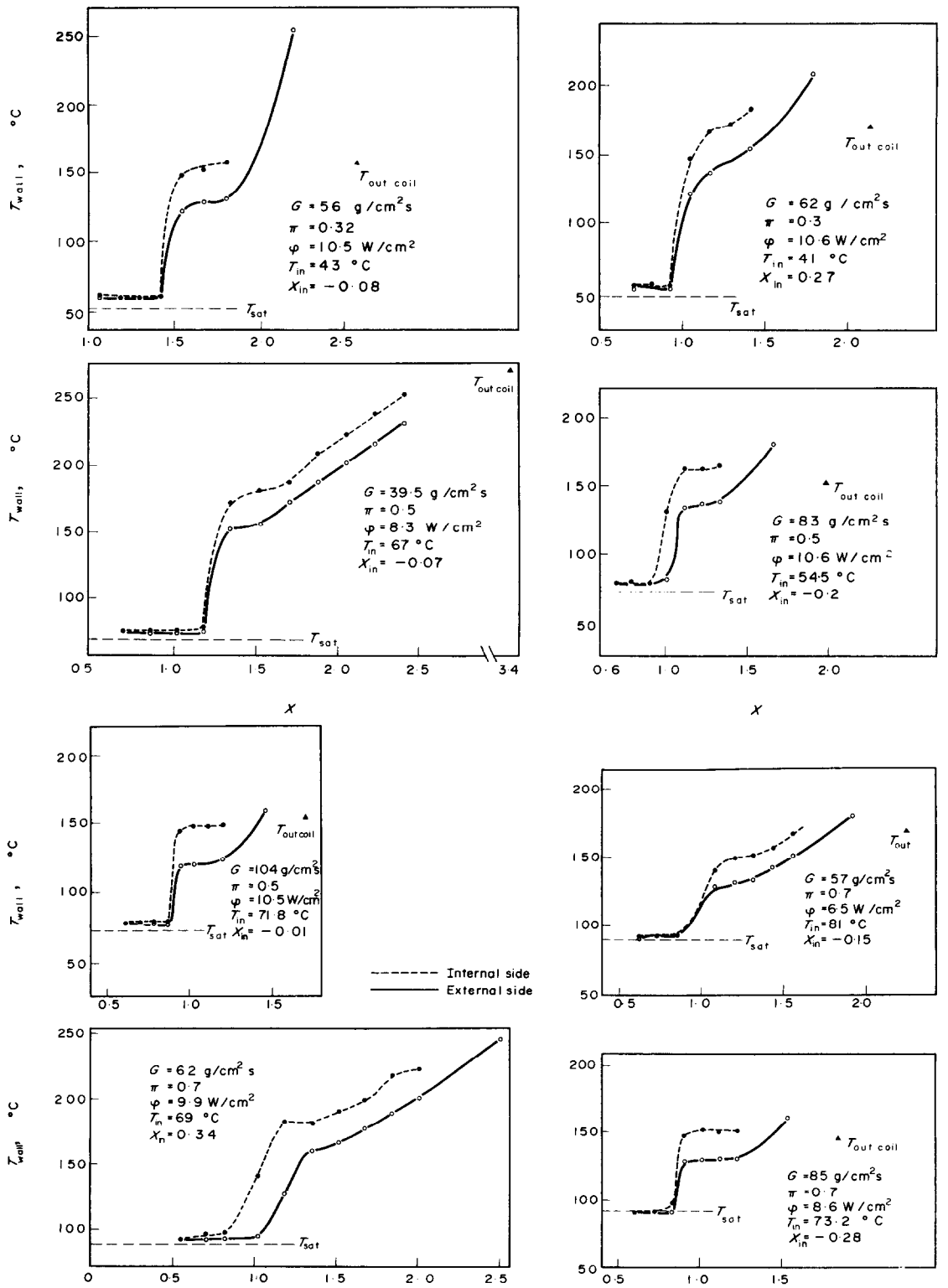
T_{wall}, °C
$T_{out\ coil}$
T_{sat}
G = 56 g/cm²s
π = 0·32
φ = 10·5 W/cm²
T_{in} = 43 °C
X_{in} = −0·08
G = 62 g/cm²s
π = 0·3
φ = 10·6 W/cm²
T_{in} = 41 °C
X_{in} = 0·27
G = 39·5 g/cm²s
π = 0·5
φ = 8·3 W/cm²
T_{in} = 67 °C
X_{in} = −0·07
G = 83 g/cm²s
π = 0·5
φ = 10·6 W/cm²
T_{in} = 54·5 °C
X_{in} = −0·2
X
G = 104 g/cm²s
π = 0·5
φ = 10·5 W/cm²
T_{in} = 71·8 °C
X_{in} = −0·01
T_{out}
G = 57 g/cm²s
π = 0·7
φ = 6·5 W/cm²
T_{in} = 81 °C
X_{in} = −0·15
Internal side
External side
G = 62 g/cm² s
π = 0·7
φ = 9·9 W/cm²
T_{in} = 69 °C
X_{in} = 0·34
G = 85 g/cm²s
π = 0·7
φ = 8·6 W/cm²
T_{in} = 73·2 °C
X_{in} = −0·28

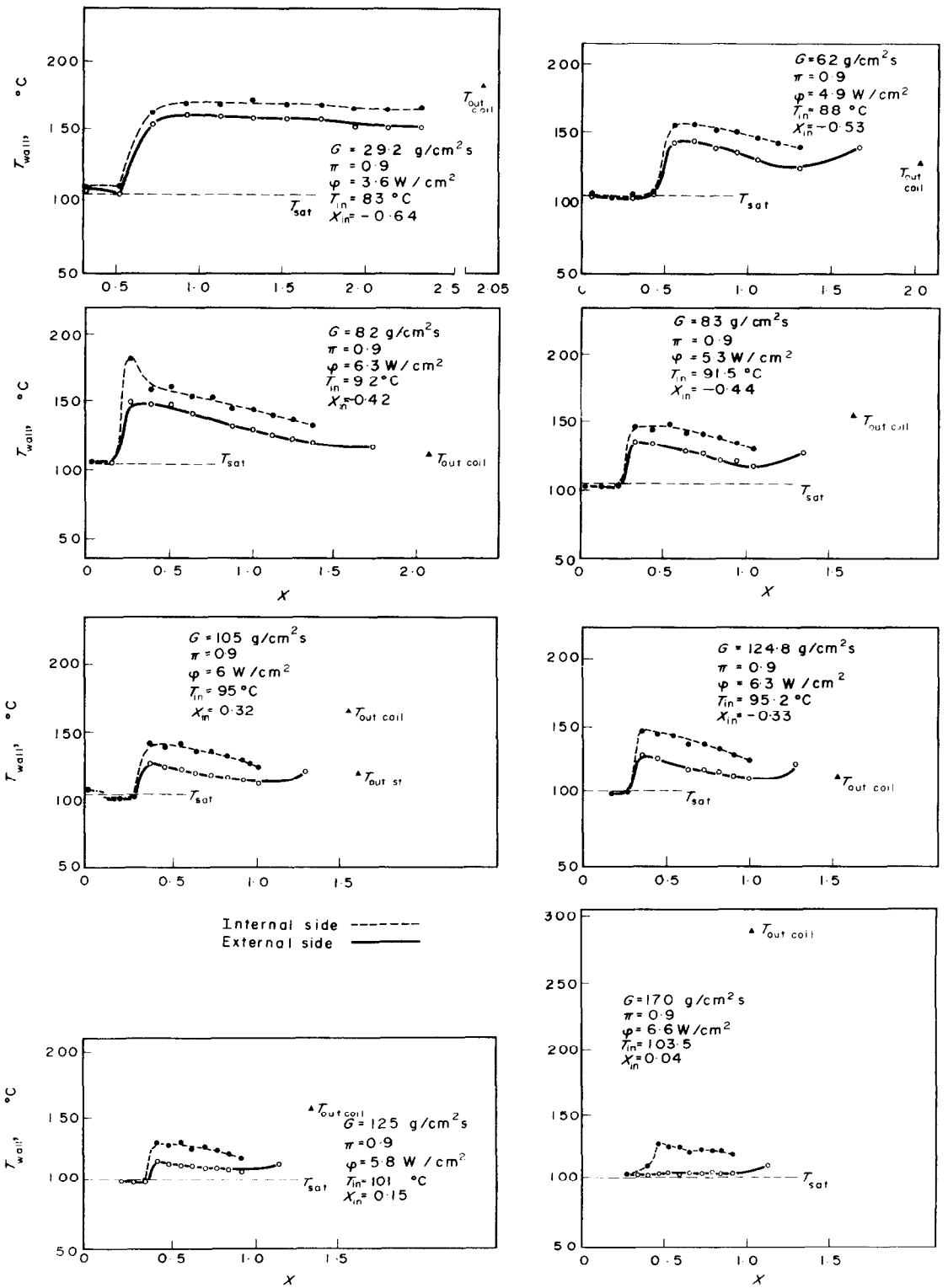

FIG. 5. External and internal wall temperature profiles in the coil at various pressures and flowrates.

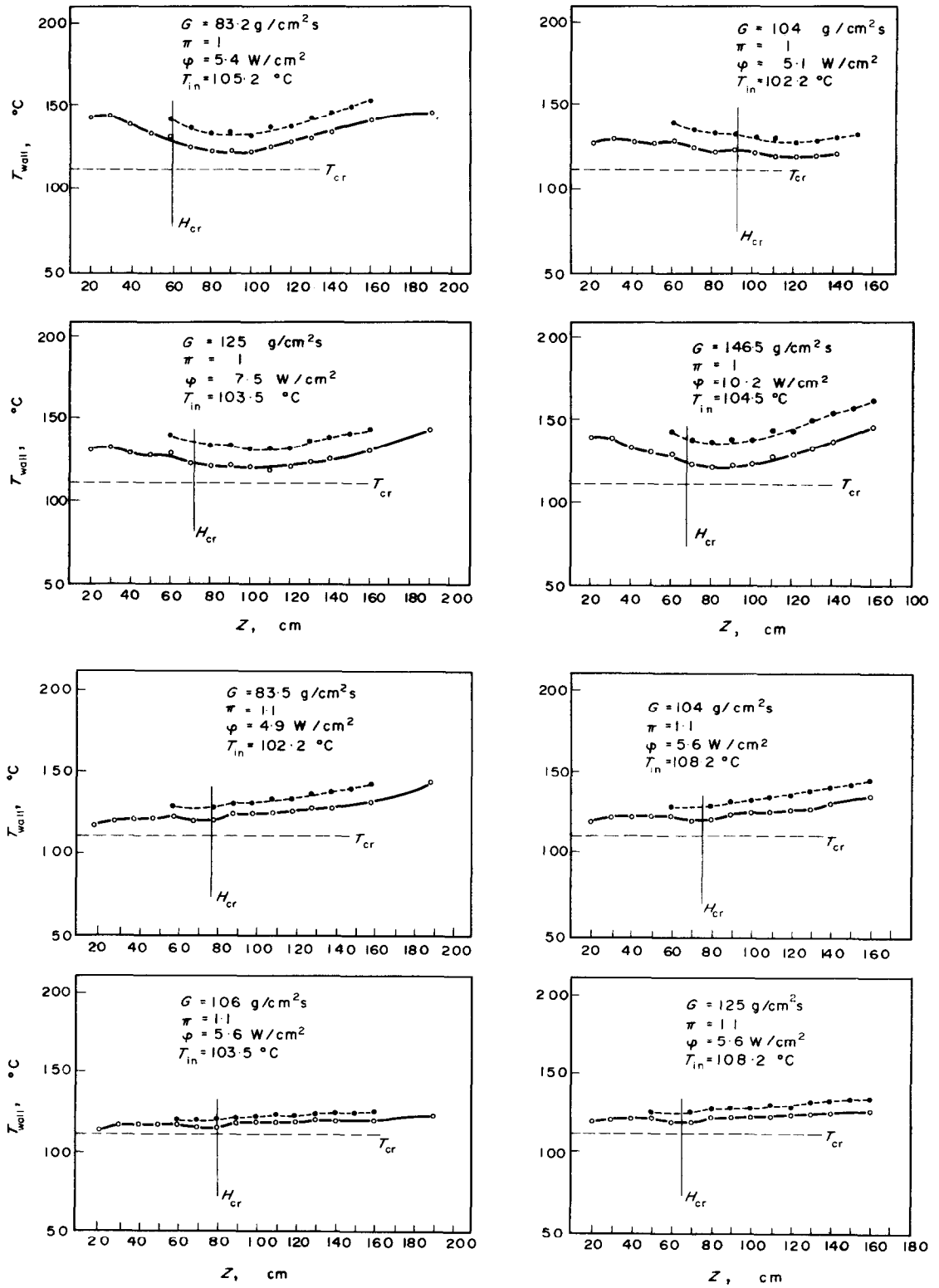

FIG. 6. External and internal wall temperature profiles in the coil at critical and hypercritical pressures.

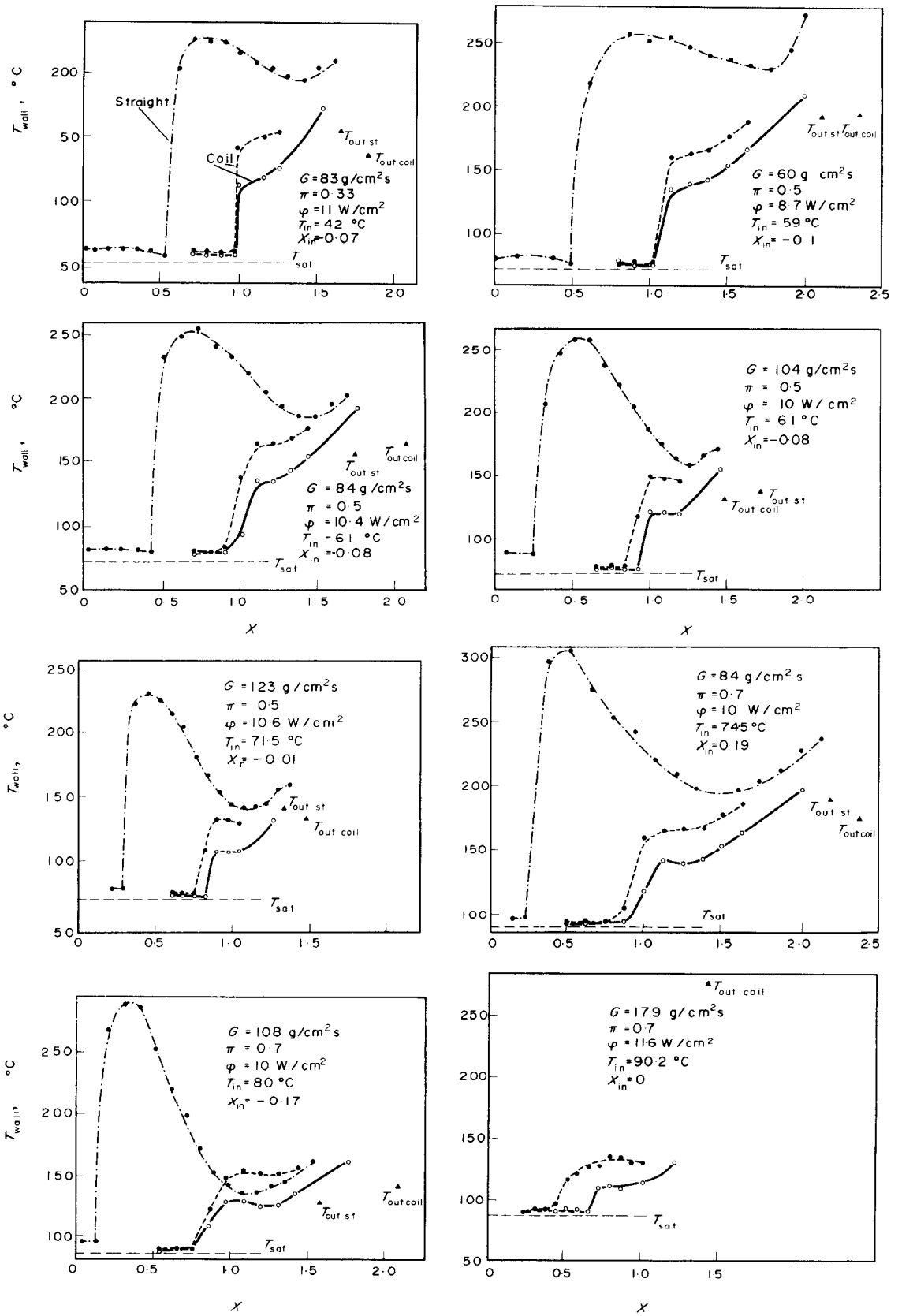

FIG. 7. Comparison of the wall temperature profiles in the straight and coiled test sections.

differentiated, but their difference is less than in sub-critical, post burnout conditions.

An overall idea of the comparison between straight and coiled ducts is provided by the diagrams of Fig. 7, in which wall temperature profiles for the same thermal and dynamic situations have been superimposed. At a first glance it appears that in straight ducts, in contrast to coils, the dry-out takes place at lower qualities (in correspondence to lower burn-out powers) and that the wall temperature rise at the dry-out is sharper and higher, thus The increase is really considerable.

Figure 8 gives an idea of this, reporting the ratio $W_{B.O\,coil}/W_{B.O\,st}$ of the burnout powers in the two test sections. The burnout powers are conventionally computed as the thermal powers injected into the test section in the heated length between the point in which the quality is $X = 0$ and the point of dry-out ($X = X_{B.O.}$), the so-called "boiling length".

The power ratio increases with the specific mass flowrate and with the pressure (between $\pi = 0{\cdot}5$ and $\pi = 0{\cdot}7$ only, the values for $\pi = 0{\cdot}9$

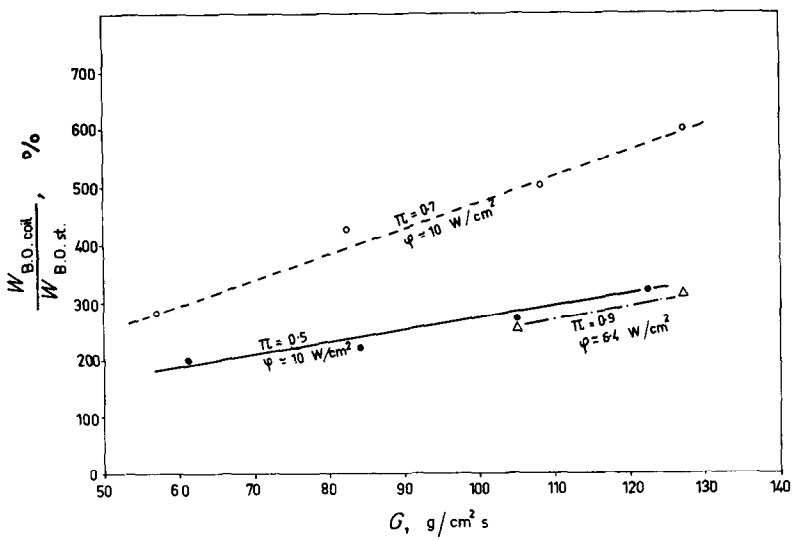

FIG. 8. Increase of burn-out power in coiled tubes ($W_{B.O\,coil}$) with respect to straight tubes ($W_{B.O.\,st}$).

indicating a quicker and worse deterioration in post burnout heat transfer.

The data collected in Figs. 4–7 are representative of a wider set of experimental data, from which the following conclusions have been drawn.

Let us consider, first of all, the increase in burn-out power which is achieved with the employment of coiled tubes in place of straight tubes. This increase is clearly due to the geometric effect of curvature, all other parameters being unchanged.

being lower). The values reached are very high, up to 500 and 600 per cent, thus showing that in heat exchangers the increase of the power exchanged along the boiling lengths (often an important fraction of the total power exchanged) is much higher in the coils, which offer a much more compact geometry. The increase in the burnout power is due obviously to a more extended boiling length.

This last increase is indicated, for some particular situations, by the graph of Fig. 9, which shows the relative gain in the burnout

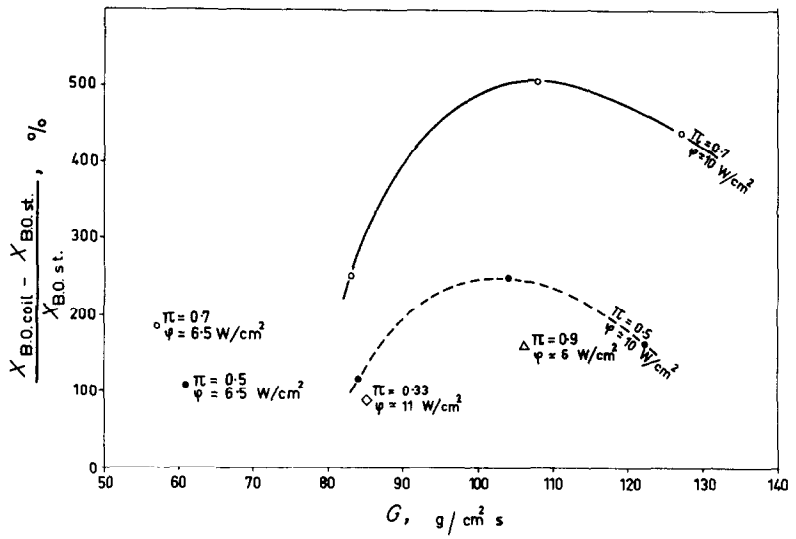

FIG. 9. Relative gain in the burn-out quality in coils with respect to straight tubes.

quality, $(X_{B.O.coil} - X_{B.O.st})/X_{B.O.st}$ vs. the specific mass flowrate for some different pressures.

While no precise statement may be deduced from the trend versus G, it may be said that this gain is of the order of some hundreds per cent (up to 500 per cent) and that, between $\pi = 0{\cdot}5$ and $\pi = 0{\cdot}7$, it increases markedly with pressure.

Another important point of comparison between coiled and straight heat exchangers is the temperature rise at the burn-out (or dry-out) point. It is well known that in once-through heat exchangers this temperature rise represents one of the most serious drawbacks. This parameter is another point in favour of coils, in the sense that the reduction in the dry-out temperature rise in the coils with respect to straight tubes (all other parameters being the same) is very considerable.

Figure 10 provides quantitative examples, giving the relative reduction, $(\Delta\theta_{B.O.st} - \Delta\theta_{B.O.coil})/\Delta\theta_{B.O.st}$, slightly increasing with the specific mass flowrate and the pressure (only between $\pi = 0{\cdot}5$ and $\pi = 0{\cdot}7$). In the cases cited in Fig. 10, the relative reduction ranges between 40 and 80 per cent. This comparison is done taking always the maximum temperature rise in the coil, i.e. that referring to the internal side.

The increase in the wall temperature, through the dry-out point, is the more dangerous (for the mechanical stresses it induces with the relative thermal expansion of the duct, concentrated corrosion, etc.) the sharper is the temperature rise, i.e. the more restricted is the length of channel of temperature rise. So, an important parameter is the slope of the curve representing the wall temperature with respect to the channel's longitudinal abscissa, Sl. In a general comparison of the thermal performances of coiled and straight tubes, the parameter Sl has also to be taken in consideration.

Figure 11 provides such a comparison, referring the relative differences in the slopes for the two cases, $(Sl_{st} - Sl_{coil})/Sl_{st}$ vs. the specific mass flowrate and for different pressures. The trends show an increase of the "gain" with G and with π, for $0{\cdot}3 \leqslant \pi \leqslant 0{\cdot}7$, the values ranging from 30 to 90 per cent. As for the temperature increases $\Delta\theta_{B.O.}$, the values of the slopes of the wall temperature profiles have been deduced, for

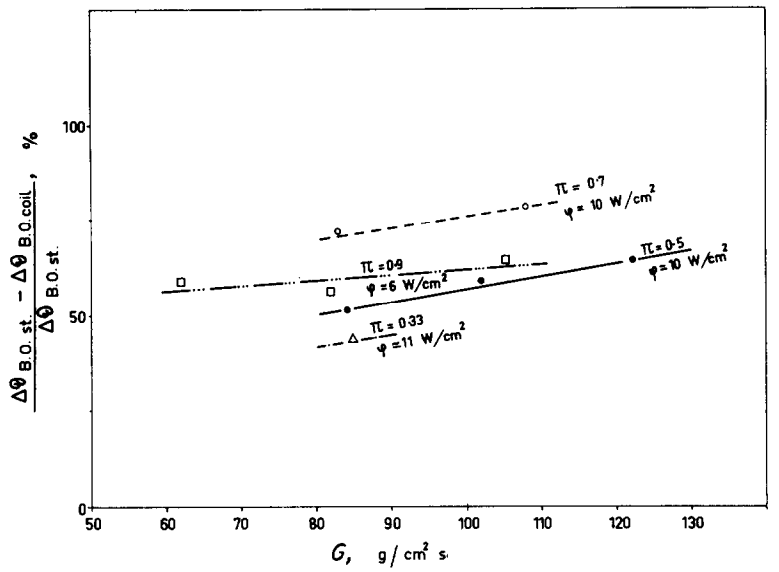

FIG. 10. Reduction of the post dry-out wall superheating in coils.

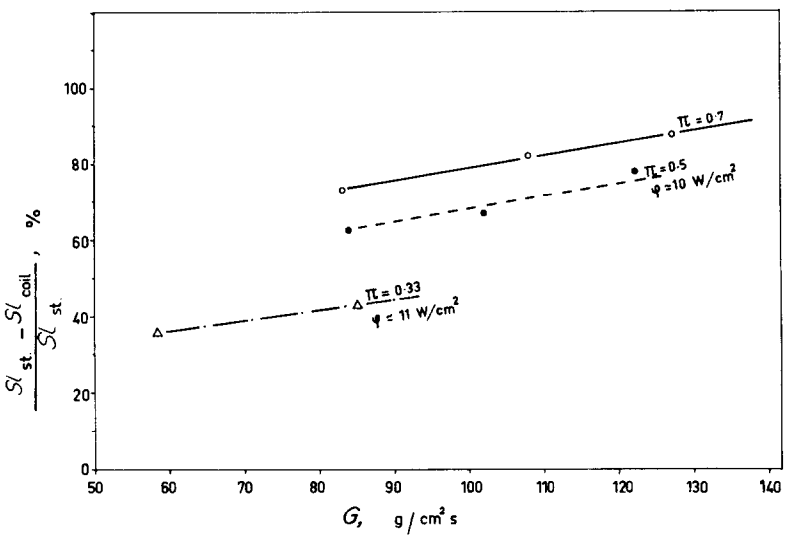

FIG. 11. Reduction of the slope of the wall temperature profile at dry-out in coils.

the coil, for the internal side temperatures whose profiles show sharper increases at the dry-out point, i.e. for the worse situation.

Let us consider now the diabatic two-phase flow in the coils and particularly the dry-out point and the post dry-out region. The diagrams of Figs. 4–7 clearly show the wall temperature profiles along the internal side and the external side of the coil. It is interesting to see what is the distance between the dry-out points along the

internal and external sides (when this detachment is experimentally revealed, the distance between two adjacent thermocouples being 10 cm).

In terms of hydraulic diameters this distance ranges from 10 to 40; in terms of quality, the constant throughout the test section. So ΔT_{os} is a significant parameter as regard the difference in cooling due to the bending of the tube. Now it is interesting to see how ΔT_{os} depends on the two main parameters which would be expected to influence the difference in internal and external

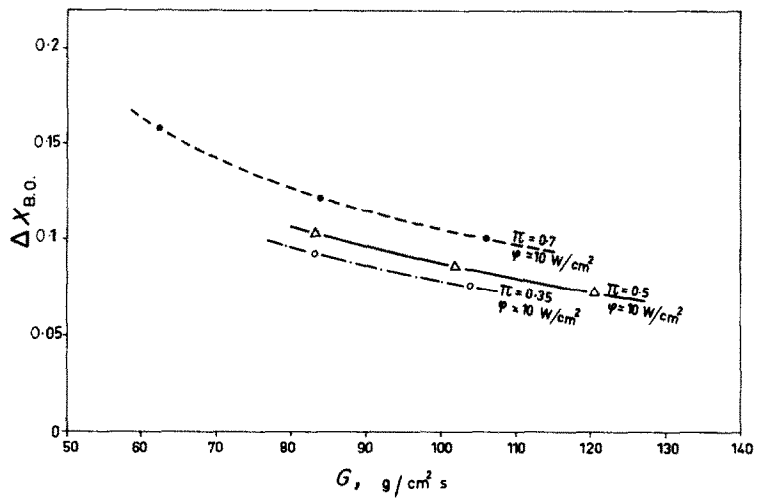

FIG. 12. Difference of dry-out qualities along the external and internal sides of the coil.

difference of the qualities at the dry-out points along the internal and external sides, $\Delta X_{B.O}$ is reported in the diagram of Fig. 12.

$\Delta X_{B.O.}$ decreases monotically versus the specific mass flowrate, and increases with pressure (for π ranging from 0·35 to 0·7); the corresponding values are small. On this profile, the results suggest that the secondary flow (which tends to make the flow situation near the internal and external sides uniform) plays an increasing role with the flowrate, in spite of the centrifugal action of separation, and with the decrease in pressure.

After the dry-out points, the internal and external side wall temperatures increase to different levels; even if these levels are not constant, the temperature difference between the two opposite sides, ΔT_{os}, remains almost

side heat transfer, namely the centrifugal acceleration of the mixture:

$$a = \frac{G^2}{\rho_m^2 R_{coil}}$$

(where ρ_m = density of the mixture, R = radius of the coil) and the reduced pressure π.

The mixture density ρ_m is often represented by the vapour density ρ_v, without an appreciable error, as the qualities of post burnout are very high. But it is difficult to compute ρ_v when the vapour superheats, as ρ_v varies appreciably with the degree of superheating. To simplify this calculation, a linear bulk temperature profile has been assumed between the point of dry-out and the outlet section (the bulk outlet temperature is recorded).

Figure 13 collects the measured ΔT_{os} (the experimental values have been corrected according to what has been reported in the preceding paragraph) versus the centrifugal acceleration.

Grouping the data at the same pressure, same mean heat flux and quality, it is possible to see that ΔT_{os} first increases with the centrifugal acceleration, reaches a maximum (10–20°C in our cases) then decreases again. This means

Let us consider now what happens when the critical pressure ($\pi = 1$) and the critical temperature are reached and surpassed through the test section (Fig. 6). Gathering three experimental values of ΔT_{os} deduced at $\pi = 1$ and $T_b = T_{cr}$, we obtain the graph of Fig. 15, which shows a linear increase of ΔT_{os} with G.

It has to be concluded that even in the thermodynamic critical point there is a temperature difference due to the bending of the tube,

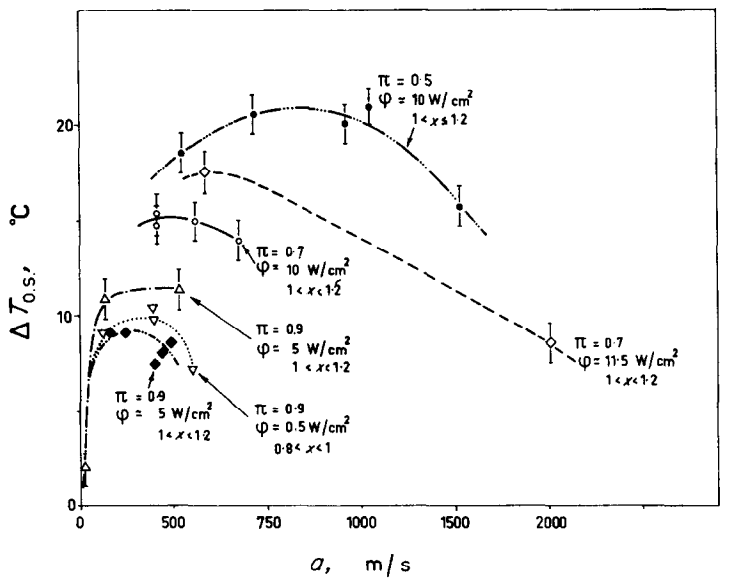

FIG. 13. Post dry-out temperature difference between the internal and external side of the coil versus the centrifugal acceleration of the mixture.

that the separating action of the centrifugal acceleration prevails against the contrary action of the secondary flow, which tends to make the mixture uniform, only for limited values of the acceleration (i.e. the flowrate) itself.

Increasing the flowrate, the secondary flow action (between the opposite sides) prevails, until ΔT_{os} disappears. Regarding the influence of pressure, Fig. 14 clearly shows the decrease of ΔT_{os} with π. Increasing π the difference between the liquid and the vapour phase gradually disappears, making the mixture uniform.

probably due to the presence of molecular clusters of different density and physical properties which are separated by the centrifuge action. However this temperature difference is relatively small if compared with that of the sub-critical two-phase flow.

The same trend appears at super-critical pressures ($\pi = 1{\cdot}1$—Fig. 6).

Finally a remark about the Miropolski and Pikus [7] post burnout heat transfer correlation for water. Figure 16 gives a comparison between experimental and computed data with Freon 12:

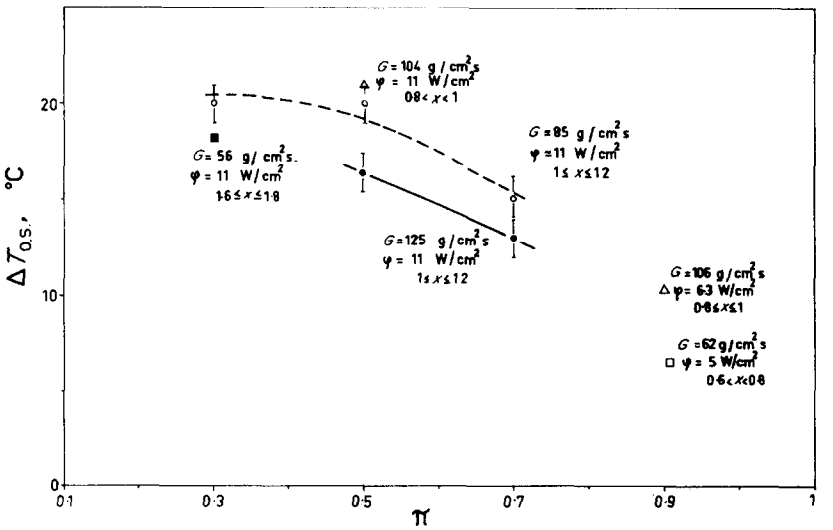

FIG. 14. Post dry-out temperature difference between the internal and external side of the coil versus the reduced pressure.

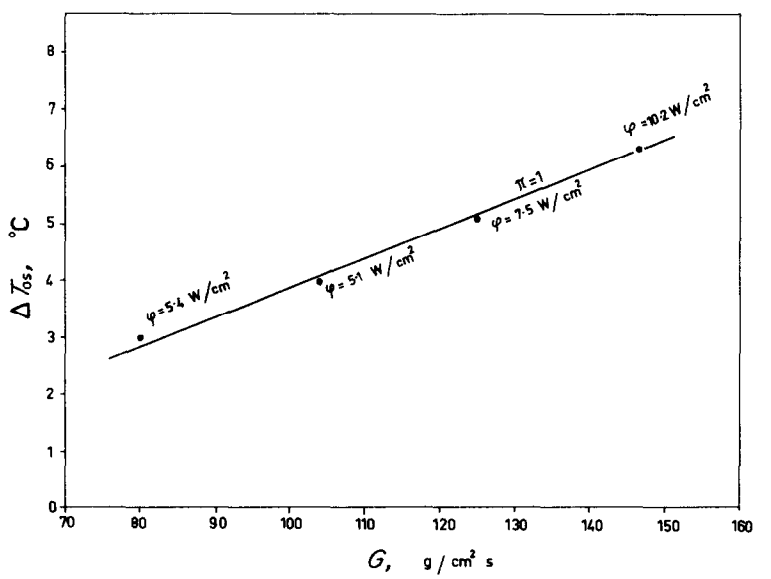

FIG. 15. Post dry-out temperature difference ΔT_{os} near the thermodynamic critical point.

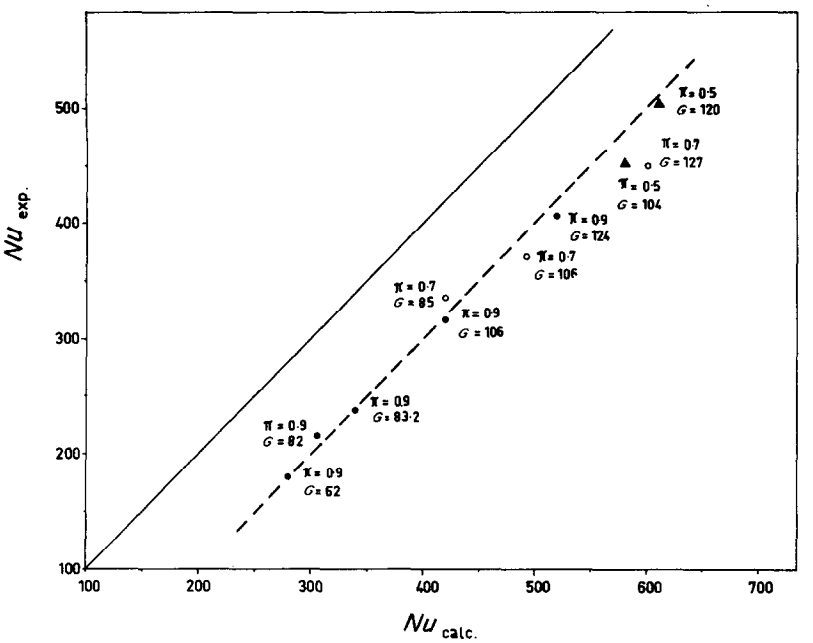

FIG. 16. Comparison of the Miropolski–Pikus post burn-out heat-transfer correlation for water with freon experimental data.

even employing the water empirical constants the scatter between theoretical and experimental Nusselt numbers is not very great and decreases increasing the absolute values of *Nu*.

CONCLUSIONS

Coiled ducts show, in comparison with straight ducts, a better two-phase flow heat transfer. The main characteristics are the following:

burn-out heat fluxes are considerably increased,

the wall temperature rises downward from the dry-out point are much smoother and lower.

In post-burnout heat transfer a wall temperature difference between the internal and the external side of the coil appears. This temperature difference remains almost constant with quality downward from the dry-out point; at first it increases, reaches a maximum, then decreases with the centrifugal acceleration in the flow; it decreases monotonically with pressure but is maintained, at critical and supercritical pressures, at a moderate level.

REFERENCES

1. Y. MORI and W. NAKAYAMA, Study on forced convective heat transfer in curved pipes, *Int. J. Heat Mass Transfer* **10**, 37–59 (1967).
2. W. H. MCADAMS, *Heat Transmission*, 3rd Ed., p. 228. McGraw Hill, New York (1954).
3. R. A. SEBAN and E. F. MCLAUGHLIN, Heat transfer in tube coils with laminar and turbulent flow, *Int. J. Heat Mass Transfer* **6**, 387–395 (1963).
4. H. F. POPPENDIEK and W. R. GAMBILL, Helical, forced-flow heat transfer and fluid dynamics in single and two-phase systems, A28/P/231, 3rd U.N. Int. Conf. on the Peaceful Uses of Atomic Energy, Geneve (1964).
5. R. C. HENDRICKS and F. F. SIMON, Heat transfer to hydrogen flowing in a curved tube. Multi-Phase Flow Symposium, ASME, New York, pp. 90–93 (1963).
6. J. R. CARVER, C. R. KAKARALA and J. S. SLOTNIK, Heat transfer in coiled tubes with two-phase flow, Report TID 20983 (31 July 1964).
7. Z. L. MIROPOLSKI and V. YU. PIKUS, Critical boiling heat fluxes in curved channels, *Heat Transfer, Sov. Res.* **1** (1), 74–79 (1969) (Krzhizhanovski Energetics Institute of Moscow).

8. A. OWHADI, K. J. BELL and G. CRAIN JR., Forced convection boiling inside helically-coiled tubes, *Int. J. Heat Mass Transfer* **2**, 1779–1793 (1968).
9. R. CHARLOT, P. PIC and R. ROUMY, Boucle Frenesie 2eme; Essais d'Assechement Critique. Sections d'Essais Hélicoidales, CEN, Grenoble, Service des Transferts Thermiques, Personal communication (1971).
10. K. J. BELL and A. OWHADI, Local heat transfer measurements during forced convection boiling in a helically coiled tube, Ist. Mech. Engrs. Symposium on Two-Phase Flow Systems. U. Leeds, Paper 7 (September. 1969).
11. K. K. SETH and E. P. STAHEL, Heat transfer from helical coils immersed in agitated vessels, *Ind. Engng. Chem.* **61**, (6), 39–49 (1969).
12. G. L. SHIRES and R. D. KHANNA, Two-phase flow and heat transfer in helical coils, Heat Transfer and Fluid Flow Research Symp., AEEW M 1023 (March 1971).
13. M. CUMO, G. E. FARELLO and G. FERRARI, Post burnout heat transfer and thermodynamic disequilibrium up to the critical pressure, 4th Int. Heat Transfer Conference, Versailles (Sept. 1970).
14. N. SPARKS and C. DILIO, *Mechanical Refrigeration*. McGraw-Hill, (1969).

INFLUENCE DE LA COURBURE SUR LE TRANSFERT THERMIQUE APRÈS ASSÈCHEMENT

Résumé—Le transfert thermique après caléfaction a été étudié comparativement dans des tubes droits et spiralés de façon à déterminer l'influence du paramètre géométrique. Du fréon 12 a été, employé jusqu'à des pressions supercritiques.

On a découvert un accroissement du transfert thermique en écoulement biphasique dans les tubes spiralés par rapport aux tubes droits, des flux thermiques de caléfaction plus élevés, des élévations de température pariétale plus douces et plus basses au point d'assèchement. Dans le transfert thermique après la caléfaction, on met en évidence une différence de température pariétale entre les côtés interne et externe de la spirale (par rapport à l'axe de l'hélice).

Cette différence de température reste pratiquement constante avec la qualité en aval du point d'assèchement et dépend de l'accélération centrifuge et de la pression de l'écoulement et garde des valeurs modérées jusqu'à des pressions supercritiques.

DER EINFLUSS DER KRÜMMUNG BEIM WÄRMEÜBERGANG NACH DER AUSTROCKNUNG

Zusammenfassung—Es wurde der Wärmeübergang nach der Austrocknung an geraden und gewendelten Rohren vergleichend untersucht, um den Einfluss der geometrischen Parameter zu klären. Als Flüssigkeit wurde Freon 12 en bis zu überkritischen Drücken verwendet. In den gewendelten Rohren zeigt sich ein intensiverer Zweiphasen-Wärmeübergang als in geraden Rohren, höhere kritische Wärmeströme, und geringere Temperaturanstiege am Austrocknungspunkt. Beim Wärmeübergang nach der Austrocknung wurde ein Unterschied in der Wandtemperatur zwischen Aussen- und Innenseite der Windungen (bezogen auf die Spiralachse) festgestellt.

Diese Temperaturdifferenz bleibt bei verändertem Dampfanteil ziemlich konstant vom Austrocknungspunkt an abwärts; sie hängt ab von der Zentrifugalbeschleunigung und vom Druck und behält ihre mässigen Werte bis zu überkritischen Drücken.

ВЛИЯНИЕ КРИВИЗНЫ НА ПЕРЕНОС ТЕПЛА В ЗАКРИТИЧЕСКОМ СОСТОЯНИИ

Аннотация—Исследовался закритический перенос тепла в прямой трубе и змеевике с тем, чтобы изучить влияние геометрического параметра. Использовался фреон-12 вплоть до сверхкритических давлений. При двухфазном течении в змеевике наблюдался более интенсивный теплообмен, чем при течении в трубе: более сильные критические тепловые потоки, более гладкие и низкие пики температуры стенки в критической точке. Определена разность температур стенки между внутренними и наружными сторонами змеевика (по отношению к оси спирали) в закритическом состоянии. Эта разность температур сохраняется почти постоянной при удалении вниз от критической точки, но зависит от центробежного ускорения течения и давления, оставаясь умеренной по своей величине вплоть до сверхкритических давлений.